Published in final edited form as:
Radiat Res. 2012 September ; 178(3): 207–216.

Murine P-glycoprotein Deficiency Alters Intestinal Injury Repair and Blunts Lipopolysaccharide-Induced Radioprotection

Elizabeth M. Staley[a,b], **Vanisha R. Yarbrough**[c], **Trenton R. Schoeb**[d], **Joseph G. Daft**[e], **Scott M. Tanner**[e], **Dennis Steverson Jr.**[e], and **Robin G. Lorenz**[a,e,1]

[a]Department of Microbiology, University of Alabama at Birmingham, Birmingham, Alabama

[b]Department of Medicine, University of Alabama at Birmingham, Birmingham, Alabama

[d]Department of Genetics, University of Alabama at Birmingham, Birmingham, Alabama

[e]Department of Pathology, University of Alabama at Birmingham, Birmingham, Alabama

[c]Department of Cellular and Molecular Biology at Harvard University, Cambridge Massachusetts

Abstract

P-glycoprotein (P-gp) has been reported to increase stem cell proliferation and regulate apoptosis. Absence of P-gp results in decreased repair of intestinal epithelial cells after chemical injury. To further explore the mechanisms involved in the effects of P-gp on intestinal injury and repair, we used the well-characterized radiation injury model. In this model, injury repair is mediated by production of prostaglandins (PGE_2) and lipopolysaccharide (LPS) has been shown to confer radioprotection. B6.*mdr1a*$^{-/-}$ mice and wild-type controls were subjected to 12 Gy total body X-ray irradiation and surviving crypts in the proximal jejunum and distal colon were evaluated 3.5 days after irradiation. B6.*mdr1a*$^{-/-}$mice exhibited normal baseline stem cell proliferation and COX dependent crypt regeneration after irradiation. However, radiation induced apoptosis was increased and LPS-induced radioprotection was blunted in the C57BL6.*mdr1a*$^{-/-}$distal colon, compared to B6 wild-type controls. The LPS treatment induced gene expression of the radioprotective cytokine IL-1α, in B6 wild-type controls but not in B6.*mdr1a*$^{-/-}$ animals. Lipopolysaccharid-induced radioprotection was absent in *IL-1R1*$^{-/-}$ animals, indicating a role for IL-1α in radioprotection, and demonstrating that P-gp deficiency interferes with IL-1α gene expression in response to systemic exposure to LPS.

INTRODUCTION

P-glycoprotein (P-gp) is the functional product of the multidrug resistance gene. It is a glycosylated transmembrane protein expressed at multiple locations including the apical surface of epithelial cells in the colon and small intestine, and epithelial cells of the pancreas, kidney and adrenal glands. P-gp is also expressed on endothelial cells at the blood brain-barrier, and on cells of hematopoietic lineage (1–3). P-gp, also known as *abcb1a*, is a member of the ATP-binding cassette super-family of transporters and is known to pump a variety of amphipathic and hydrophobic substrates from the intracellular environment (4, 5). P-gp overexpression is often seen in tumors and its expression can be induced by multiple chemotherapeutic agents, leading to acquired resistance to treatment due to its ability to

[1]Address for correspondence: Department of Pathology, University of Alabama at Birmingham, 1825 University Blvd., SHEL 602, Birmingham, AL 35294-2182; rlorenz@uab.edu.

Editor's note. The online version of this article (DOI: 10.1667/RR2835.1) contains supplementary information that is available to all authorized users.

pump these drugs out of the cytoplasm (6, 7). Expression of multidrug resistance gene polymorphisms has been associated with development of inflammatory bowel disease (IBD) in specific patient populations (8–11). Introduction of the P-gp deficiency onto the C57BL/6 animal model renders these mice susceptible to induction of intestinal inflammation by epithelial disruption secondary to chemical damage, indicating a role for multidrug resistance gene expression in maintaining intestinal homeostasis and injury repair (12). Interestingly, P-gp has also been associated with mitigating apoptotic resistance. Kidney proximal tubules cells were shown to be protected from induced apoptosis as a result of increased P-gp expression (13), and *in vitro* studies using blast cells have shown that over-expression of multidrug resistance gene correlates with increased cell survival and decreased apoptosis (14).

The relationship between proliferation and apoptosis is critical in the gastrointestinal tract, where the epithelium exists in a state of continuous regeneration maintained by multipotent stem cells found at the base of intestinal crypts. Stem cells divide and produce daughter stem cells, or highly proliferative transit cells (15, 16). Transit cells migrate to the proliferative zone found in the lower portion of each crypt and further divide and differentiate to produce mature epithelial cells (17). Mature epithelial cells then migrate onto the intestinal villi where they remain, unless damaged, for anywhere from 3 to 5 days before dying and being sloughed off into the intestinal lumen (18, 19).

The best characterized model for studying injury repair and intestinal epithelial maintenance is radiation-induced injury (17, 20, 21). Radiation injury targets rapidly dividing cells by inducing DNA damage and causing cell cycle arrest and apoptosis. High doses of radiation effectively eliminate rapidly dividing cells in the crypt proliferative zone, and denude the intestinal epithelium. Regeneration of the intestinal barrier then becomes the responsibility of crypt stem cells (17, 20, 21). Crypt regeneration following radiation injury has been shown to be dependent on induction of cyclooxygenase 1 (COX1) and subsequent synthesis of prostaglandin E_2 (PGE_2) (22). Prostaglandins are lipid mediators known to play an integral role in multiple biological processes such as wound healing and blood clotting, and are known to be crucial for the maintenance of the intestinal mucosa (23–26).

One method for attenuation of apoptosis induced by acute radiation injury is the systemic administration of lipopolysaccharide (LPS). Lipopolysaccharide administration stimulates the innate immune response and has been shown to confer radioprotective benefits as a result of a TNFα/TNFR1 dependent increase in COX2 expression and subsequent synthesis of PGE_2 (27). In accordance with these studies LPS is also known to increase the level of intestinal P-gp. However, it has also been postulated that P-gp expression may be integral to the cellular response to bacterial stimuli, extruding bacterial ligands from the intracellular environment prior to stimulation of innate pattern recognition receptors (28). It is unclear whether LPS would have a radioprotective effect on animals deficient in P-gp expression and whether these mice would have normal epithelial repair after radiation injury. We have used P-gp deficient B6.*mdr1a*$^{-/-}$ mice to study these questions and to determine the molecules involved in injury repair in this model. Our data show that the level of P-gp significantly impacts the levels of epithelial cell apoptosis after radiation exposure and blunts the ability of LPS to protect the epithelium from radiation damage. In the B6 model, this LPS-induced protection is mediated by the cytokine IL-1α and we now make the novel observation that expression of this cytokine is decreased in the absence of P-gp expression.

MATERIALS AND METHODS

Animals

C57BL/6J-*Abcba1*^{tm1Bor}*N10* (B6.*mdr1a*$^{-/-}$) was derived as previously described under a research crossbreeding agreement with Taconic Farms, Germantown, NY (12). B6.*129S7-Il1r1*$^{tm1Imx/J}$ is commercially available from Jackson Laboratories. However, these animals were a kind gift from Dr. David Chaplin of the University of Alabama at Birmingham and have been backcrossed 10 times to the C57BL/6 background. The Institutional Care and Use Committee of the University of Alabama at Birmingham approved all experiments and all animals were housed in ventilated racks (Thoren Caging Systems, Inc., Hazleton, PA). All caging, bedding, water and food were sterilized prior to use. The detailed list of our facility's SPF conditions can be accessed at http://main.uab.edu/sites/ComparativePathology/surveillance/.

Irradiation and Tissue Harvest

Male mice were subjected to lethal (12 Gy) doses of X-ray irradiation at 8–12 weeks old in the X-RAD 320 irradiator (Precision X-Ray Inc., N. Branford, CT), in accordance with previous studies evaluating cellular regeneration and repair. Animals were sacrificed at either 6 h (apoptotic studies) or 3.5 days (crypt regeneration studies) after lethal irradiation. Colon and proximal jejunum were harvested and fixed in Bouin's solution (Fisher, Pittsburgh, PA). Tissue was then cut into 5 mm segments and embedded longitudinally in paraffin to allow for cross-sectional analysis. The distal ileum was harvested and placed in RNA Later (Ambion®, Austin, TX) prior to RNA isolation.

LPS and Indomethacin Treatment

B6.*mdr1a*$^{-/-}$ and B6 animals were given i.p. injections of 0.5 mg/kg LPS (*Escherichia coli* 0111:B4, Sigma) dissolved in sterile pyrogen free PBS (Mediatech, Manassas, VA), or PBS alone 24 h prior to irradiation. Indomethacin (Sigma) was dissolved at 12.5 mg/ml into 70% ethanol and further diluted in 5% sterile PBS prior to use. B6 and B6.*mdr1a*$^{-/-}$ animals were treated with 1.5 mg/kg indomethacin i.p. every 8 h beginning 14 h prior to irradiation.

Crypt Survival Microcolony Assay

Proliferating/regenerating cells were identified based on 5-bromodeoxyuridine (BrdUrd) (Sigma) incorporation and detection as described by Cohn *et al*. (29). Crypt regeneration was quantified in animals 3.5 days after irradiation as described previously (27). Animals were injected i.p. with BrdUrd 90 min prior to sacrifice. Tissue was fixed at sacrifice using cold Bouin's Fixative. Paraffin embedded tissue sections were sliced in 5 um sections and deparaffinized using Citrisolv. Exposing slides to 2N hydrochloric acid for 30 min denatured cellular DNA. Non-specific protein binding sites were blocked through incubation in blocking buffer containing 1% bovine serum albumin fraction V, 0.2% non-fat powdered dry milk (Nestle, Vevey, Switzerland), and 0.3% Triton-X 100 dissolved in PBS. BrdUrd incorporation was detected using a polyclonal goat anti-BrdUrd antibody (a kind gift of Dr. S. M. Cohn of the University of Virginia) diluted in blocking buffer and incubated at 4°C overnight (29). BrdUrd incorporation was detected using a Cy3 labeled donkey anti-goat antibody (Jackson ImmunoResearch, West Grove, PA), and nuclei were stained using Hoechst bisbenzimide 33258 (Sigma). Cellular regeneration was assessed by fluorescence microscopy using the Zeiss Axioskop 2 (Carl Zeiss Inc., Thornwood, NY). A regenerative crypt was defined as containing at least 5 cells demonstrating BrdUrd incorporation. An average of 6 intestinal cross-sections were analyzed per mouse.

Apoptosis

Cellular apoptosis was visually confirmed by microscopy to determine the presence of characteristic morphological changes such as cellular fragmentation, cell shrinkage, margination, and chromatin condensation. To quantify apoptotic cells, tissue sections were exposed to terminal deoxynucleotidyl transferase mediated dUTP nick end labeling (TUNEL) using the ApopTag apoptosis kit from Millipore (Billerica, MA). Hoechst bisbenzimide was used to label nuclei. To further characterize caspase 3 activity, slides were deparaffinized and rehydrated in PBS. Antigen retrieval was then performed using citrate buffer (1.8 m*M* Citric acid, and 8.3 m*M* sodium citrate in deionized water) and slides were blocked in a solution of 3% hydrogen peroxide and PBS. Expression of Avidin and Biotin was blocked using the kit from Vector Laboratories (Burlingame, CA). Non-specific protein binding sites were blocked prior to an overnight incubation in buffer containing the polyclonal rabbit anti-cleaved caspase 3 antibody (Cell Signaling Technology, Danvers, MA). The antibody was further labeled with streptavidin-HRP (Jackson ImmunoResearch Laboratories, Inc., West Grove, PA) and then visualization was achieved using TSA™Cyanine 3 Tyramide (Perkin Elmer, Boston, MA). Three-to-six intestinal sections were captured for each animal using a 20× objective lens and the SPOT Insight® digital camera (Diagnostic Instruments, Inc., Sterling Heights, MI). To quantify apoptotic cells, the green channel image of the crypts was extracted, the threshold was assessed, and the image was inverted to convert TUNEL staining nuclei to black objects on a white background using Image Pro Plus® v6 image analysis software (Media Cybernetics, Inc., Bethesda, MD). Total nuclei were quantified similarly using blue channel images. Apoptotic data was presented as the ratio of the area of TUNEL staining to the area of Hoechst staining. Caspase 3 activity was similarly assessed using the red channel image for cells labeled by the cleaved caspase 3 antibody.

RNA Isolation and Quantitative Real-Time Reverse-Transcriptase Polymerase Chain Reaction

RNA was isolated from distal ileal tissue using TRIzol® as described by Sacchi *et al.* (Invitrogen, Carlsbad, CA) (30). Quantitative real-time reverse-transcriptase polymerase chain reaction was performed using Applied Biosystems gene specific primer probe sets in combination with TaqMan Universal PCR Mix (Invitrogen) as previously described (12). Data were analyzed by the “delta-delta Ct” relative quantitation method as described in Applied Biosystems manufacturer’s instructions (4371095 Rev A, PE Applied Biosystems, Foster City, CA). The average crossing threshold of the housekeeping gene (18S) is subtracted from the average crossing threshold of each target gene to determine the relative expression (ΔCt). To determine fold change, experimental animal data was compared to the control (as implied in the figure legends) for each gene. Upper and lower limits of the average fold change were determined using the standard deviation of the ΔCt of the experimental group in the $2^{\Delta\Delta Ct}$ formula, as outlined in the manufacturer’s protocol.

PGE_2 ELISA

PGE_2 production after irradiation was quantified using the Prostaglandin E_2 EIA Kit available from Cayman Chemical (Ann Arbor, MI). Tissue from the proximal ileum was harvested at sacrifice and snap frozen in liquid nitrogen until use. Tissue was weighed prior to mechanical disruption in 5 mls homogenization buffer (0.1 *M* phosphate buffer containing 1 m*M* EDTA, 10 μ*M* indomethacin). Protein was diluted 1:400 and applied to the ELISA plate as directed. Sample was detected at a range of 1.0–0.078 ng/ml. Protein was expressed as ng/mg of homogenized tissue.

Statistical Analysis

Statistical analysis was performed using the QuickCalcs program available from GraphPad (La Jolla, CA). Statistical analysis on crypt regeneration data sets was performed using the Kruskal-Wallis test, and Dunn's multiple comparison analysis. Quantitative real-time reverse-transcriptase polymerase chain reaction data was analyzed between individual data sets by using an unpaired Student's *t* test. Analysis of quantitative real-time reverse-transcriptase polymerase chain reaction data was conducted using the differences in detectable fluorescent emission crossing thresholds between genes of interest and housekeeping genes.

RESULTS

Radiation-Induced Apoptosis, and Intestinal Crypt Regeneration in Small Intestinal Tissue

Radiation targets rapidly dividing cells by damaging DNA resulting in mitotic or apoptotic death (17, 20, 21). It has been previously shown that over-expression of P-gp increases cellular resistance to apoptosis (13, 14). Therefore, B6.*mdr1a*$^{-/-}$ P-gp deficient animals may demonstrate an increased susceptibility to radiation damage as a result of altered rates of apoptosis and subsequent aberrant cell cycling. To examine levels of apoptosis in the intestinal epithelium after radiation injury, B6.*mdr1a*$^{-/-}$ and B6 control animals were lethally irradiated and sacrificed 6 h after irradiation. Apoptosis, as detected by TUNEL, was increased after lethal irradiation in both the B6 and B6.*mdr1a*$^{-/-}$ animals, but this increase was only significant in the B6.*mdr1a*$^{-/-}$ proximal jejunum (Fig. 1A–C). In addition, B6.*mdr1a*$^{-/-}$ animals demonstrated no significant increase in apoptotic area at baseline when compared to wild-type controls (Fig. 1C). To confirm the involvement of caspase signaling pathway in this radiation model tissue was labeled with antibody targeting expression of cleaved caspase 3. Cleaved caspase 3 immunoreactivity confirmed TUNEL results, and B6.*mdr1a*$^{-/-}$ animals demonstrated increased labeling of cleaved caspase 3 in intestinal tissue after exposure to radiation (data not shown).

Next, we assessed whether this altered apoptosis in intestinal epithelial tissue corresponded with increased cellular proliferation, potentially rendering cells more susceptible to radiation-induced cell death (31). To assess basal levels of epithelial cell proliferation, animals were injected with BrdUrd 90 min prior to sacrifice. BrdUrd incorporation into cells during DNA synthesis was evaluated in unmanipulated B6.*mdr1a*$^{-/-}$ and wild-type control animals. Interestingly, there was no significant difference in baseline cellular proliferation between control and P-gp deficient animals (11.9 ± 1.6 BrdUrd-positive nuclei/crypt in B6 versus 11.0 ± 2.3 in B6.*mdr1a*$^{-/-}$) at baseline.

Death of crypt epithelial cells renders intestinal villi unable to repopulate after radiation damage, and impairs the ability of the intestinal epithelium to repair itself after injury. B6.*mdr1a*$^{-/-}$ and wild-type control animals were exposed to lethal doses of irradiation (12 G), and sacrificed 3.5 days later to evaluate crypt regeneration. Regenerative crypts were quantified as those containing at least 5 BrdUrd positively labeled nuclei (Fig. 1D and E). B6.*mdr1a*$^{-/-}$animals demonstrated no significant change in crypt regeneration after radiation injury when compared to B6 control animals (Fig. 1F).

Radiation-Induced Apoptosis, and Intestinal Crypt Regeneration in Distal Colonic Tissue

Previously reported cellular apoptosis assays, as well as crypt regeneration assays have been conducted almost solely on small intestinal tissue, with little work being carried out that investigates colonic tissue (22). Because P-gp is expressed in the jejunum, our initial experiments were designed to characterize the effects of *mdr1a* gene deficiency in small intestinal tissue. However, P-gp expression increases along the cephalocaudal axis of the

gastrointestinal (GI) tract similarly to gastrointestinal bacterial load, with expression increasing distally toward the colon (3, 32). To assess the effects of P-gp deficiency where its absence may initiate more profound disturbances to cellular homeostasis, we next chose to examine apoptosis and crypt regeneration in distal colonic tissue. The decision to conduct our experiments in both small intestinal and colonic tissue enabled us to compare our results with current literature, and also draw correlations between P-gp expression and function.

Experiments were conducted as described above using tissue from the distal colon. In distal colonic tissue, we again demonstrated an increase in epithelial apoptosis in response to radiation-induced injury in B6 animals deficient in P-gp expression (Fig. 2A). This data supports previously published results indicating a role for P-gp expression in moderating cellular apoptosis. However, B6.*mdr1a*$^{-/-}$ and B6 control animals demonstrated no differences in rates of colonic crypt regeneration after radiation injury (Fig. 2B). Interestingly, colonic crypt regeneration in both animal strains was much lower than values seen in small intestinal tissue (Fig. 2B compared to Fig. 1F). This data indicates that P-gp deficiency alone does not impair normal crypt regenerative ability after acute radiation-induced injury, however it does induce apoptosis, presumably in the crypt proliferative zone.

PGE_2 and Crypt Regeneration after Acute Radiation Injury

Previous studies using FVB/N female mice have shown that crypt regeneration after radiation injury corresponds with increased intestinal *COX1* levels and requires production of PGE_2 (27). To evaluate whether the B6 male animal model was operating by the same pathway, B6.*mdr1a*$^{-/-}$ and B6 control animals were evaluated for expression of intestinal *COX1* mRNA expression and PGE_2 levels. To evaluate these parameters in the same mice where crypt regeneration was assessed, RNA was isolated from distal ileal tissue and quantitative real-time reverse-transcriptase polymerase chain reaction is performed (Fig. 3A). Data is presented as changes from baseline gene expression in B6 control animals after normalization for 18S expression. PGE_2 expression is quantified by ELISA on extracts from proximal ileal tissue (Fig. 3B). In accordance with previous publications, B6 animals demonstrated a modest increase in *COX1* expression, however, this did not translate to a significant increase in PGE_2 protein production. Interestingly, B6.*mdr1a*$^{-/-}$ animals showed significantly increased levels of both *COX1* and PGE_2 after exposure to radiation, although crypt regeneration in these animals was not significantly enhanced when compared to B6 controls (Fig. 3A–B, Fig. 2B and Fig. 1F). This data suggests that crypt regeneration after radiation-induced injury may not be solely contingent upon production of PGE_2 in our animal model, and/or that PGE2 production does not directly correlate with absolute numbers of regenerating crypts.

To ascertain whether PGE_2 production was necessary for crypt regeneration after radiation injury, B6 and B6.*mdr1a*$^{-/-}$ animals were treated with the non-specific COX inhibitor indomethacin to block all stimuli inducing production of PGE_2, prior to exposure to radiation. Administration of indomethacin ameliorated production of PGE_2 (data not shown). The elimination of PGE_2 production resulted in significantly reduced crypt regeneration in distal colonic tissue in B6.*mdr1a*$^{-/-}$ animals, in fact crypt regeneration was completely abrogated in these animals (the ratio of crypt regeneration in indomethacin treated animals to non-treated animals was 0). While crypt regeneration in control B6 animals was reduced, the reduction was not significant (the ratio of crypt regeneration in indomethacin treated animals to non-treated animals was 0.6) (Fig. 3C). This data confirms that as previously reported in the FVB/N mice, PGE_2 production plays a role in crypt regeneration after irradiation in the B6 and B6.*mdr1a*$^{-/-}$ animal models. However, it does not seem to be the sole factor involved in crypt regeneration in the B6 animal model (Fig. 3C).

LPS Induced Radioprotection of Intestinal Tissue

Systemic LPS stimulation has been shown to induce crypt regeneration in the small intestine after radiation-induced injury (22). Furthermore, it has been shown to increase the expression and activity of P-gp (33). LPS-induced radioprotection may be mediated via this increase in P-gp expression and consequently, radioprotection should be abrogated in P-gp deficient animals. To investigate the effects of LPS treatment on crypt regeneration in B6.*mdr1a*$^{-/-}$ we injected P-pg deficient and wild-type animals with LPS 24 h prior to irradiation. To assess crypt regeneration across a spectrum of P-gp expression, proximal jejunal and distal colonic tissue was analyzed. Animals were irradiated and sacrificed as described above, and crypt regeneration was quantified. B6.*mdr1a*$^{-/-}$ and B6 controls both displayed increased levels of crypt regeneration in the proximal jejunum following systemic treatment with LPS prior to exposure to radiation (Fig. 4A). However, this radioprotection was abrogated in the distal colon of the B6.*mdr1a*$^{-/-}$ (Fig. 4B), indicating the P-gp plays an integral role in the colonic response to systemic LPS stimulation.

LPS Induced Expression of TNFα and COX Enzymes

LPS-induced radioprotection in female FVB/N mice is mediated by increased production of TNFα, which subsequently induces expression of *COX2* and production of PGE_2 (27). As previously published studies have shown that increased COX2 expression enhances P-gp expression, we hypothesized that this LPS radioprotection pathway would not function normally in the B6.*mdr1a*$^{-/-}$mice (34). We therefore wanted to assess the levels of LPS-induced expression of *TNF*α and *COX2* in P-pg deficient animals following acute radiation injury. In B6 animals, exposure to radiation significantly elevated gene expression of *TNF*α and *COX2*, compared to non-treated animals (Fig. 5). However, when LPS was administered no significant alteration of gene expression of *TNF*α or *COX2* in B6 animals was noted (Fig. 5). Slightly different results were seen in B6.*mdr1a*$^{-/-}$ animals, where exposure to radiation significantly increased expression of *TNF*α, but not *COX2*. However, as was seen in the B6 controls, LPS administration dampened this increased expression of *TNF*α (Fig. 5). LPS did not alter baseline production of PGE2 in nonirradiated B6 or B6.*mdr1a*$^{-/-}$proximal ileum (data not shown). These results indicate that while induced PGE_2 expression appears to play a critical role in baseline crypt regeneration after radiation injury in B6.*mdr1a*$^{-/-}$ animals (Fig 3), it does not play a role in LPS induced radioprotection in male B6 control animals.

LPS Induces Radioprotection and Innate Immune Cytokines

As B6 male control animals appeared to use a pathway independent of TNFα induced PGE_2 production/COX2 for LPS-induced radioprotection, we began to investigate alternative mechanisms of LPS-induced protection. We examined gene expression of innate inflammatory cytokines known to effect injury repair in the GI tract: IL-1α, IL-1β, IL10 and IFNγ (35–39). Evaluation of their expression in male B6 control mice after LPS-induced radioprotection demonstrated that only IL-1α expression was increased after LPS pretreatment and subsequent radiation (Supplementary Table 1; http://dx.doi.org/10.1667/RR2835.1.S2 and Fig. 6A). Additionally, B6 animals expressed significantly more IL-1α when LPS was administered prior to irradiation, compared to B6.*mdr1a*$^{-/-}$ animals (Fig. 6A). This data correlates with the diminished crypt regeneration following LPS treatment in B6.*mdr1a*$^{-/-}$ animals, and indicates a potential role for IL-1α in promoting enhanced radioprotection in male B6 animals after pretreatment with LPS.

Role of IL-1α in LPS-Induced Radioprotection

To confirm the importance of IL-1α in LPS induced crypt regeneration, B6.*IL-1R1*$^{-/-}$ animals were evaluated for crypt regeneration after administration of LPS and exposure to

radiation. Animals deficient in IL-1 receptor expression demonstrated a slight increase in crypt regeneration when compared to B6 and B6.*mdr1a*$^{-/-}$ animals after exposure to radiation (Fig. 6B compared to Fig. 4B). However, like B6.*mdr1a*$^{-/-}$ animals, B6.*IL-1R1*$^{-/-}$ animals showed no evidence of LPS induced radioprotection (Fig. 6B compared to Fig. 4B). This data confirms that recognition of IL-1α is critical in LPS induced radioprotection in B6 animals.

DISCUSSION

FVB.129P2-Abcba1^{tmBor}N7 (FVB.*mdr1a*$^{-/-}$) mice develop a spontaneous unremitting colitis when maintained in a specific pathogen-free environment and disease has been proven to be ameliorated by both prophylactic and therapeutic antibiotic treatment (28). FVB.*mdr1a*$^{-/-}$ demonstrate altered phosphorylation patterns of junctional proteins, which are associated with decreased intestinal tissue resistance early in development, and prior to development of clinical symptoms of colitis (40).

Recently we demonstrated that re-derivation of the *mdr1a* gene deficiency onto the C57BL/6 background strain ameliorates development of spontaneous disease (12). Furthermore, B6.*mdr1a*$^{-/-}$ animals demonstrated no alterations to intestinal tissue integrity and ion permeability (unpublished data from the Lorenz lab). However, B6.*mdr1a*$^{-/-}$ animals proved to be more susceptible to colitis induction when exposed to chemically induced epithelial disruption, which highlights a role for P-gp expression in regulating epithelial homeostasis and injury repair (12).

To elucidate the role P-gp plays in epithelial injury repair, we examined the effects of low dose radiation injury on B6.*mdr1a*$^{-/-}$ mice. It was our hypothesis that animals deficient in P-gp expression would succumb more readily to radiation-induced tissue damage as a result of altered epithelial homeostasis. As predicted B6.*mdr1a*$^{-/-}$ animals failed to recover from radiation-induced injury, implicating a role for P-gp expression in epithelial injury repair after radiation-induced damage (unpublished data, Lorenz and Staley).

Studies of multidrug resistance gene expression in humans have indicated that the multidrug resistance protein plays a role in regulating cellular apoptosis. P-gp expression and function has been strongly associated with increased resistance to spontaneous apoptosis (14). The most highly characterized method of studying intestinal apoptosis and epithelial cell regeneration uses acute radiation-induced injury of proximal jejunum. To investigate the role of P-gp expression in cellular turnover, we initially used this small intestinal model because it enabled us to compare our results with previous studies. However, our true experimental focus was the effects of injury in the distal colon, where normal epithelial P-gp expression is highest and where the effects of P-gp deficiency should be the most profound.

Apoptosis was evaluated in P-pg deficient mice and control animals under both irradiated and nonirradiated conditions. Only B6.*mdr1a*$^{-/-}$ distal colonic tissue showed significantly increased epithelial apoptosis after acute radiation injury when compared to control animals. Previous reports have correlated increased epithelial apoptosis in response to acute injury with poor crypt regenerative capabilities after injury (20). To evaluate the effects of increased apoptosis on tissue regeneration, crypt microcolony formation was assessed in wild-type and P-pg deficient animals after exposure to lethal doses of X-ray irradiation. We observed no significant reduction in proximal jejunal or distal colonic crypt regeneration in B6.*mdr1a*$^{-/-}$ animals. This data suggests that the baseline epithelial regeneration is not effected by P-gp deficiency.

Baseline proximal jejenal crypt regeneration in FVB/N female mice has been previously shown to be dependent on increased *COX1* expression and subsequent PGE_2 production

(41). Although radiation induced an increase in *COX1* gene expression in both B6 control and P-pg deficient mice, an increase in the level of PGE_2 was only seen in the proximal ileum of the irradiated B6.*mdr1a*$^{-/-}$, and not in the B6. Therefore, it appeared that this mechanism might not function in our model as previously reported for the FVB/N female mice. We chose to further investigate this pathway by evaluating the effects of *COX* inhibition on crypt regeneration. Indomethacin treatment completely abrogated distal colonic crypt regeneration in B6.*mdr1a*$^{-/-}$ mice, and did not significantly reduce crypt regeneration in B6 control animals. These data demonstrated that COX enzymes and PGE_2 production are critical in the B6.*mdr1a*$^{-/-}$ response to radiation-induced injury, but other pathways appear to contribute to this regeneration in the male B6 model.

Systemic LPS exposure has been shown to induce increased crypt regeneration after radiation injury by production of TNFα, stimulation of TNFR1, and subsequent induction of COX expression and PGE_2 synthesis (27). As increased COX2 expression enhances P-gp expression, we hypothesized that this LPS radioprotection pathway would not function normally in the B6.*mdr1a*$^{-/-}$ mice (34, 42). Crypt regeneration data indicated that, while B6 control and B6.*mdr1a*$^{-/-}$ animals both demonstrated increased crypt regeneration after pre-exposure to LPS, the magnitude of the response was significantly muted in P-gp mice, particularly in distal colonic tissue. In the distal colon, LPS conferred a fivefold increase in crypt regeneration in B6 animals, while B6.*mdr1a*$^{-/-}$ animals demonstrated only a 1.5-fold increase.

To evaluate key downstream modulators of the LPS-induced radioprotection pathway, we demonstrated that irradiation did induce increased expression of *TNF*α and *COX* enzymes. However, LPS treatment prior to irradiation attenuated this response in control and B6.*mdr1a*$^{-/-}$animals. Again, as discussed above, this data differs from that previously published on female FVB/N mice (27, 42). One potential reason for this difference could be that we used male mice of a different strain in our experiments. In preliminary experiments, we found that nonirradiated female B6 mice expressed significantly higher levels of both *COX2* (12.11-fold increase, range 4.88–30.57), and *mdr1a* (35.07-fold increase, range 9.68–126.98) than their male littermates. This altered baseline expression of two of the genes involved in this pathway could clearly account for the difference seen in our male data when compared to previously published data on female mice. Our data indicates that TNFα induction of *COX2* expression is not the pathway used for LPS-induced radioprotection in the male B6 model. Therefore, LPS may be inducing radioprotection through an alternative pathway.

To further investigate alternative mechanisms for LPS-induced radioprotection we chose to investigate levels of regulatory (IL10) and inflammatory (IL-1α, IL-1β, IFNγ) cytokines previously reported to play a role in the repair of radiation-induced injury. Our gene expression data indicated that intestinal IFNγ, IL-1β and IL10 are not altered after systemic LPS-treatment and subsequent radiation injury, and therefore they would not appear to be part of the alternative mechanism seen in LPS-induced radioprotection in male B6 animals. However, we found that, when B6 animals are treated with LPS prior to exposure to radiation, they express significantly increased intestinal levels of IL-1α. Given previous reports that IL-1α can induce COX2 expression in intestinal epithelial cell lines, we hypothesized that this IL-1α/COX2/PGE_2 pathway could be playing a role in radiation-induced injury repair in our B6 model (43). We chose to further investigate the role of IL-1 gene expression on LPS-induced radioprotection by using animals deficient in expression of type 1 IL-1 receptor (44). IL-1R1 is known as the IL-1 signaling receptor (IL-1R2 being the decoy receptor), and has been shown to bind both IL-1α and IL-1β, with a tenfold greater affinity for IL-1α (45, 46). We were able to demonstrate that animals deficient in expression of IL-R1 displayed crypt regeneration similar to wild-type animals after exposure to

radiation. Additionally, we demonstrated that LPS-induced radioprotection is reduced in animals deficient in expression of IL-1R1. This data clearly indicates the importance of IL-1 in LPS-induced radioprotection in the B6 male model of radiation injury repair. As B6.*mdr1a*$^{-/-}$ mice do not show this increased intestinal expression of IL-1α after systemic LPS treatment and radiation injury, we can conclude that P-gp is involved in the mechanism of LPS-induced expression of IL-1α after radiation damage.

In summary, decreased expression of P-gp results in increased rates of intestinal epithelial cell apoptosis and diminished LPS-induced injury-repair mechanisms secondary to inadequate induction of the radioprotective cytokine IL-1α (Supplementary Fig. 1; http://dx.doi.org/10.1667/RR2835.1.S1). This mechanism may be one contributing factor to the increased susceptibility of humans with decreased expression of P-gp or P-gp deficient mice to colonic inflammation after chemical and bacterial epithelial injury.

Supplementary Material

Refer to Web version on PubMed Central for supplementary material.

Acknowledgments

We would like to thank Peggy R. McKie-Bell and Jamie L. McNaught for their assistance and members of the Lorenz lab for their valuable advice. This work was supported in part by the NIH grants R01 DK059911, P01 DK071176, and the Molecular Pathology and Imaging Core of the University of Alabama at Birmingham Digestive Diseases Research Development Center (P30 DK064400). EMS received partial salary support from T32 AI07051. An NIH/NIDDK StepUP Fellowship supported VRY. SMT received partial salary support from a Crohn's and Colitis Student Research Fellowship Award, and from the UAB-Hughes Med to Grad Fellowship. Aspects of this project were conducted in biomedical research space that was constructed with funds supported in part by the NIH grant C06RR020136.

References

1. Cordon-Cardo C, O'Brien JP, Casals D, Rittman-Grauer L, Biedler JL, Melamed MR, et al. Multidrug-resistance gene (p-glycoprotein) is expressed by endothelial cells at blood-brain barrier sites. Proc Natl Acad Sci USA. 1989; 86:695–8. [PubMed: 2563168]
2. Klimecki WT, Futscher BW, Grogan TM, Dalton WS. P-glycoprotein expression and function in circulating blood cells from normal volunteers. Blood. 1994; 83:2451–8. [PubMed: 7513198]
3. Thiebaut F, Tsuruo T, Hamada H, Gottesman MM, Pastan I, Willingham MC. Cellular localization of the multidrug-resistance gene product p-glycoprotein in normal human tissues. Proc Natl Acad Sci USA. 1987; 84:7735–8. [PubMed: 2444983]
4. Fromm MF. P-glycoprotein: A defense mechanism limiting oral bioavailability and cns accumulation of drugs. Int J Clin Pharmacol Ther. 2000; 38:69–74. [PubMed: 10706193]
5. Mizutani T, Masuda M, Nakai E, Furumiya K, Togawa H, Nakamura Y, et al. Genuine functions of p-glycoprotein (abcb1). Curr Drug Metab. 2008; 9:167–74. [PubMed: 18288958]
6. Goldstein LJ, Galski H, Fojo A, Willingham M, Lai SL, Gazdar A, et al. Expression of a multidrug resistance gene in human cancers. J Natl Cancer Inst. 1989; 81:116–24. [PubMed: 2562856]
7. Chaudhary PM, Roninson IB. Induction of multidrug resistance in human cells by transient exposure to different chemotherapeutic drugs. J Natl Cancer Inst. 1993; 85:632–9. [PubMed: 8096875]
8. Fiedler T, Buning C, Reuter W, Pitre G, Gentz E, Schmidt HH, et al. Possible role of mdr1 two-locus genotypes for young-age onset ulcerative colitis but not crohn's disease. Eur J Clin Pharmacol. 2007; 63:917–25. [PubMed: 17665184]
9. Ho GT, Soranzo N, Nimmo ER, Tenesa A, Goldstein DB, Satsangi J. Abcb1/mdr1 gene determines susceptibility and phenotype in ulcerative colitis: Discrimination of critical variants using a gene-wide haplotype tagging approach. Hum Mol Genet. 2006; 15:797–805. [PubMed: 16434479]

10. Onnie CM, Fisher SA, Pattni R, Sanderson J, Forbes A, Lewis CM, et al. Associations of allelic variants of the multidrug resistance gene (abcb1 or mdr1) and inflammatory bowel disease and their effects on disease behavior: A case-control and meta-analysis study. Inflamm Bowel Dis. 2006; 12:263–71. [PubMed: 16633048]
11. Potocnik U, Ferkolj I, Glavac D, Dean M. Polymorphisms in multidrug resistance 1 (mdr1) gene are associated with refractory crohn disease and ulcerative colitis. Genes Immun. 2004; 5:530–9. [PubMed: 15505619]
12. Staley EM, Schoeb TR, Lorenz RG. Differential susceptibility of p-glycoprotein deficient mice to colitis induction by environmental insults. Inflamm Bowel Dis. 2009; 15:684–96. [PubMed: 19067430]
13. Thevenod F, Friedmann JM, Katsen AD, Hauser IA. Up-regulation of multidrug resistance p-glycoprotein via nuclear factor-kappab activation protects kidney proximal tubule cells from cadmium-and reactive oxygen species-induced apoptosis. J Biol Chem. 2000; 275:1887–96. [PubMed: 10636889]
14. Pallis M, Turzanski J, Higashi Y, Russell N. P-glycoprotein in acute myeloid leukaemia: Therapeutic implications of its association with both a multidrug-resistant and an apoptosis-resistant phenotype. Leuk Lymphoma. 2002; 43:1221–8. [PubMed: 12152989]
15. Bjerknes M, Cheng H. The stem-cell zone of the small intestinal epithelium. I. Evidence from paneth cells in the adult mouse. Am J Anat. 1981; 160:51–63. [PubMed: 7211716]
16. Cheng H, Leblond CP. Origin, differentiation and renewal of the four main epithelial cell types in the mouse small intestine. V. Unitarian theory of the origin of the four epithelial cell types. Am J Anat. 1974; 141:537–61. [PubMed: 4440635]
17. Potten CS, Loeffler M. Stem cells: Attributes, cycles, spirals, pitfalls and uncertainties. Lessons for and from the crypt. Development. 1990; 110:1001–20. [PubMed: 2100251]
18. Gavrieli Y, Sherman Y, Ben-Sasson SA. Identification of programmed cell death in situ via specific labeling of nuclear DNA fragmentation. J Cell Biol. 1992; 119:493–501. [PubMed: 1400587]
19. Hall PA, Coates PJ, Ansari B, Hopwood D. Regulation of cell number in the mammalian gastrointestinal tract: The importance of apoptosis. J Cell Sci. 1994; 107 (Pt 12):3569–77. [PubMed: 7706406]
20. Potten CS. A comprehensive study of the radiobiological response of the murine (bdf1) small intestine. Int J Radiat Biol. 1990; 58:925–73. [PubMed: 1978853]
21. Potten CS, Loeffler M. A comprehensive model of the crypts of the small intestine of the mouse provides insight into the mechanisms of cell migration and the proliferation hierarchy. J Theor Biol. 1987; 127:381–91. [PubMed: 3328018]
22. Houchen CW, Stenson WF, Cohn SM. Disruption of cyclooxygenase-1 gene results in an impaired response to radiation injury. Am J Physiol Gastrointest Liver Physiol. 2000; 279:G858–65. [PubMed: 11052981]
23. Dubois RN, Abramson SB, Crofford L, Gupta RA, Simon LS, Van De Putte LB, et al. Cyclooxygenase in biology and disease. Faseb J. 1998; 12:1063–73. [PubMed: 9737710]
24. Newberry RD, McDonough JS, Stenson WF, Lorenz RG. Spontaneous and continuous cyclooxygenase-2-dependent prostaglandin e2 production by stromal cells in the murine small intestine lamina propria: Directing the tone of the intestinal immune response. J Immunol. 2001; 166:4465–72. [PubMed: 11254702]
25. Newberry RD, Stenson WF, Lorenz RG. Cyclooxygenase-2-dependent arachidonic acid metabolites are essential modulators of the intestinal immune response to dietary antigen. Nat Med. 1999; 5:900–6. [PubMed: 10426313]
26. Wallace JL, Ma L. Inflammatory mediators in gastrointestinal defense and injury. Exp Biol Med. 2001; 226:1003–15.
27. Riehl TE, Newberry RD, Lorenz RG, Stenson WF. Tnfr1 mediates the radioprotective effects of lipopolysaccharide in the mouse intestine. Am J Physiol Gastrointest Liver Physiol. 2004; 286:G166–73. [PubMed: 14525729]

28. Panwala CM, Jones JC, Viney JL. A novel model of inflammatory bowel disease: Mice deficient for the multiple drug resistance gene, mdr1a, spontaneously develop colitis. J Immunol. 1998; 161:5733–44. [PubMed: 9820555]
29. Cohn SM, Lieberman MW. The use of antibodies to 5-bromo-2′-deoxyuridine for the isolation of DNA sequences containing excision-repair sites. J Biol Chem. 1984; 259:12456–62. [PubMed: 6490625]
30. Chomczynski P, Sacchi N. Single-step method of rna isolation by acid guanidinium thiocyanate-phenol-chloroform extraction. Anal Biochem. 1987; 162:156–9. [PubMed: 2440339]
31. Booth D, Potten CS. Protection against mucosal injury by growth factors and cytokines. J Natl Cancer Inst Monogr. 2001:16–20. [PubMed: 11694560]
32. Mouly S, Paine MF. P-glycoprotein increases from proximal to distal regions of human small intestine. Pharm Res. 2003; 20:1595–9. [PubMed: 14620513]
33. Moriguchi J, Kato R, Nakagawa M, Hirotani Y, Ijiri Y, Tanaka K. Effects of lipopolysaccharide on intestinal p-glycoprotein expression and activity. Eur J Pharmacol. 2007; 565:220–4. [PubMed: 17399699]
34. Patel VA, Dunn MJ, Sorokin A. Regulation of mdr-1 (p-glycoprotein) by cyclooxygenase-2. J Biol Chem. 2002; 277:38915–20. [PubMed: 12138126]
35. Bass H, Mosmann T, Strober S. Evidence for mouse th1- and th2-like helper t cells in vivo. Selective reduction of th1-like cells after total lymphoid irradiation. J Exp Med. 1989; 170:1495–511. [PubMed: 2572669]
36. Hancock SL, Chung RT, Cox RS, Kallman RF. Interleukin 1 beta initially sensitizes and subsequently protects murine intestinal stem cells exposed to photon radiation. Cancer Res. 1991; 51:2280–5. [PubMed: 2015592]
37. Johnke RM, Smith ES, Cariveau MJ, Evans MJ, Kilburn JM, Bakken NT, et al. Radioprotection of murine gastrointestinal epithelium by interleukin-1alpha involves down-regulation of the apoptotic response. Anticancer Res. 2008; 28:3601–7. [PubMed: 19189640]
38. Wu SG, Miyamoto T. Radioprotection of the intestinal crypts of mice by recombinant human interleukin-1 alpha. Radiat Res. 1990; 123:112–5. [PubMed: 2371377]
39. Bharhani MS, Borojevic R, Basak S, Ho E, Zhou P, Croitoru K. Il-10 protects mouse intestinal epithelial cells from fas-induced apoptosis via modulating fas expression and altering caspase-8 and flip expression. Am J Physiol Gastrointest Liver Physiol. 2006; 291:G820–9. [PubMed: 17030898]
40. Resta-Lenert S, Smitham J, Barrett KE. Epithelial dysfunction associated with the development of colitis in conventionally housed mdr1a−/− mice. Am J Physiol Gastrointest Liver Physiol. 2005; 289:G153–62. [PubMed: 15774938]
41. Cohn SM, Schloemann S, Tessner T, Seibert K, Stenson WF. Crypt stem cell survival in the mouse intestinal epithelium is regulated by prostaglandins synthesized through cyclooxygenase-1. J Clin Invest. 1997; 99:1367–79. [PubMed: 9077547]
42. Riehl T, Cohn S, Tessner T, Schloemann S, Stenson WF. Lipopolysaccharide is radioprotective in the mouse intestine through a prostaglandin-mediated mechanism. Gastroenterology. 2000; 118:1106–16. [PubMed: 10833485]
43. Hinterleitner TA, Saada JI, Berschneider HM, Powell DW, Valentich JD. Il-1 stimulates intestinal myofibroblast cox gene expression and augments activation of cl- secretion in t84 cells. Am J Physiol. 1996; 271:C1262–8. [PubMed: 8897833]
44. Glaccum MB, Stocking KL, Charrier K, Smith JL, Willis CR, Maliszewski C, et al. Phenotypic and functional characterization of mice that lack the type i receptor for il-1. J Immunol. 1997; 159:3364–71. [PubMed: 9317135]
45. Arend WP, Malyak M, Smith MF Jr, Whisenand TD, Slack JL, Sims JE, et al. Binding of il-1 alpha, il-1 beta, and il-1 receptor antagonist by soluble il-1 receptors and levels of soluble il-1 receptors in synovial fluids. J Immunol. 1994; 153:4766–74. [PubMed: 7963543]
46. Sims JE, Gayle MA, Slack JL, Alderson MR, Bird TA, Giri JG, et al. Interleukin 1 signaling occurs exclusively via the type i receptor. Proc Natl Acad Sci USA. 1993; 90:6155–9. [PubMed: 8327496]

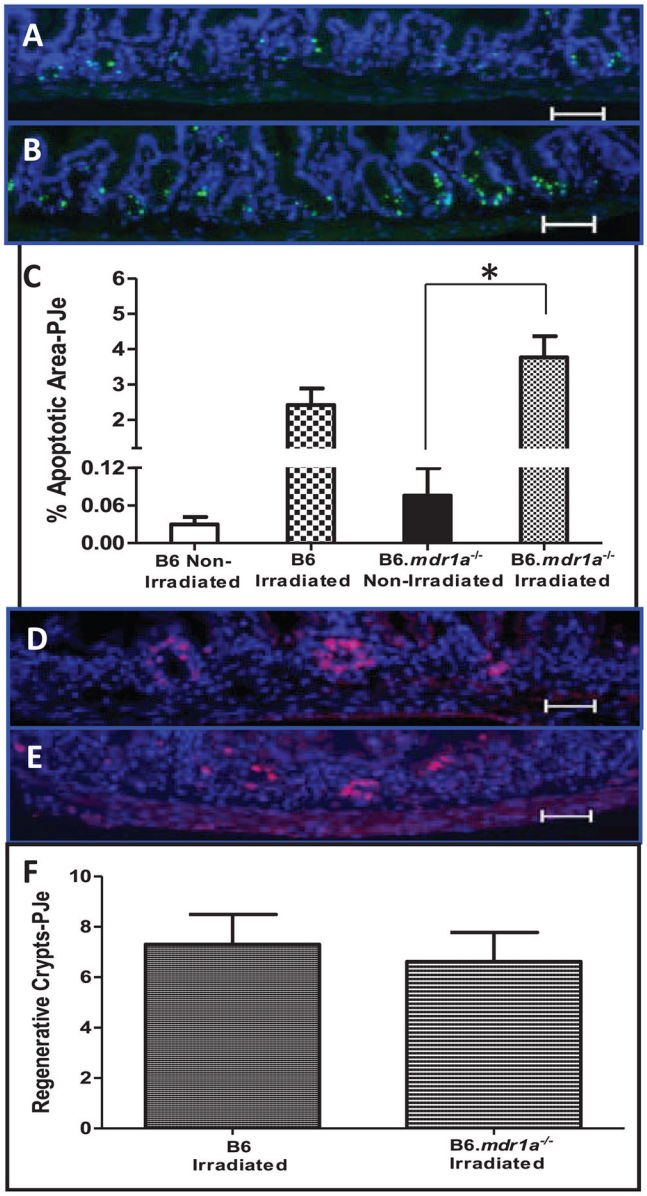

FIG. 1.

Radiation-induced apoptosis and intestinal crypt regeneration in small intestinal tissue. Apoptosis was assessed in proximal jejunal tissue from B6 (panel A), and B6.*mdr1a*$^{-/-}$ (panel B) animals. Apoptotic cells were labeled by TUNEL and nuclei were labeled using Hoechst dye (blue). Apoptosis is quantified as the ratio of apoptotic area to area of nuclear stain (panel C). Crypt regeneration was assessed in proximal jejunal tissue from B6 (panel D), and B6.*mdr1a*$^{-/-}$ (panel E) animals. Crypt regeneration was quantified as a crypt containing a minimum of 5 BrdUrd positive cells, 6 cross-sections were counted/animal. Data are presented as the average number of regenerative crypts/cross-section (panel F). All groups contained at least $N = 5$ animals. Images were captured at a 200×magnification, Bar =0.5 μm. *$P < 0.05$ between treatment groups.

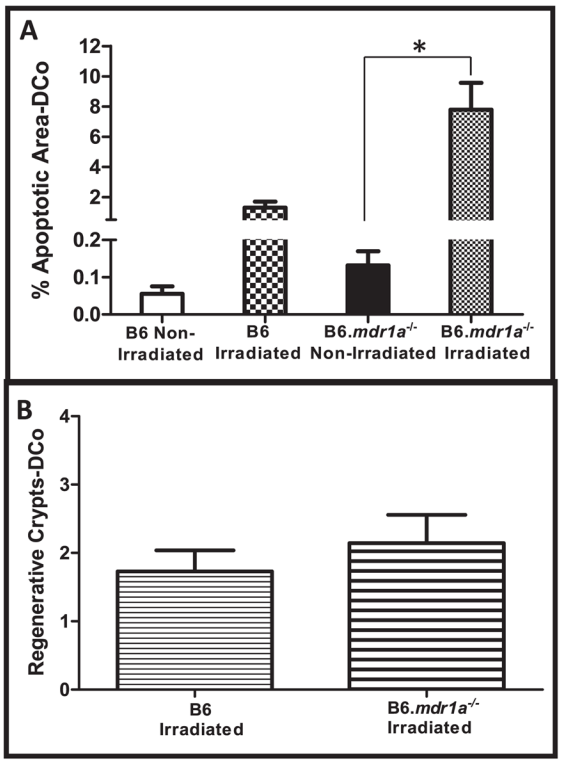

FIG. 2.

Radiation-induced apoptosis and intestinal crypt regeneration in distal colonic tissue (DCo). Apoptosis was assessed in tissue from B6 and B6.*mdr1a*$^{-/-}$ animals as previously described. Apoptosis is quantified as the ratio of apoptotic area to area of nuclear stain (panel A). Crypt regeneration was assessed in tissue from B6 and B6.*mdr1a*$^{-/-}$animals as previously described. Data is presented as the average number of regenerative crypts/cross-section (panel B). All groups contained at least N=5 animals. *P < 0.05 between treatment groups.

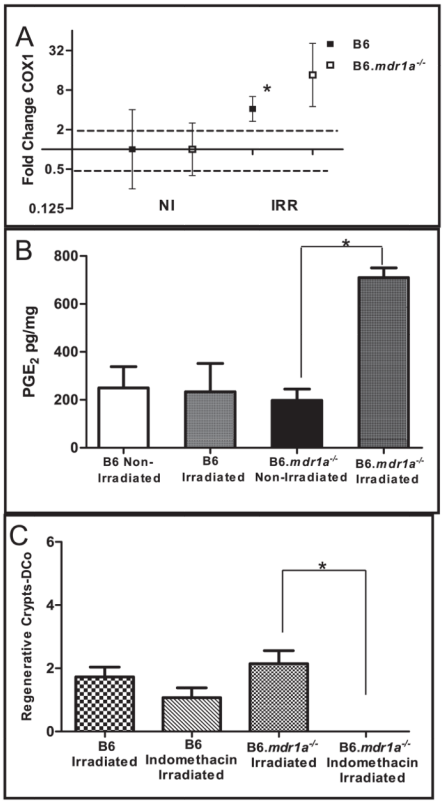

FIG. 3.

Levels of COX1 and PGE_2 in B6 and B6.*mdr1a*$^{-/-}$ animals. Range for gene expression data (panel A) was calculated from the standard deviation of the ΔΔCT value and the average gene expression is plotted with upper and lower limits of the range shown. Dotted lines demonstrate the range of physiological relevance. ELISA (panel B) determined PGE_2 content in the proximal ileum. Distal colonic (DCo) tissue was harvested and analyzed for crypt regeneration (panel C). $N = 5$ animals for all groups except B6 irradiated LPS where $N = 3$. $*P < 0.05$ between treatment groups.

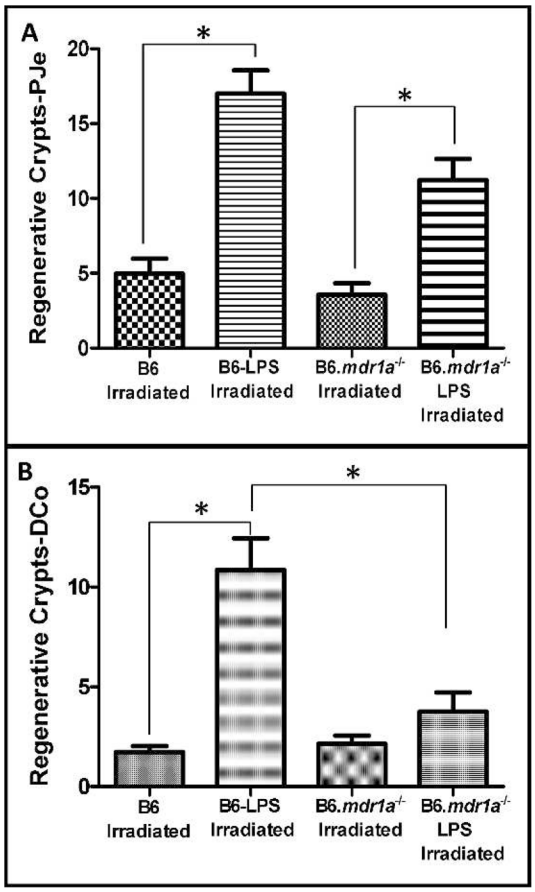

FIG. 4.

Crypt regeneration in lethally irradiated and LPS-treated mice. B6 and B6.*mdr1a*$^{-/-}$ animals were injected with LPS prior to exposure to lethal doses of X-ray radiation. Crypt regeneration was quantified as described. Data is presented as the average number of regenerative crypts/cross-section. All groups contained at least $N = 5$ animals, except B6 irradiated LPS where N =3. Bar = 0.5 lm. *$P < 0.05$ between treatment groups.

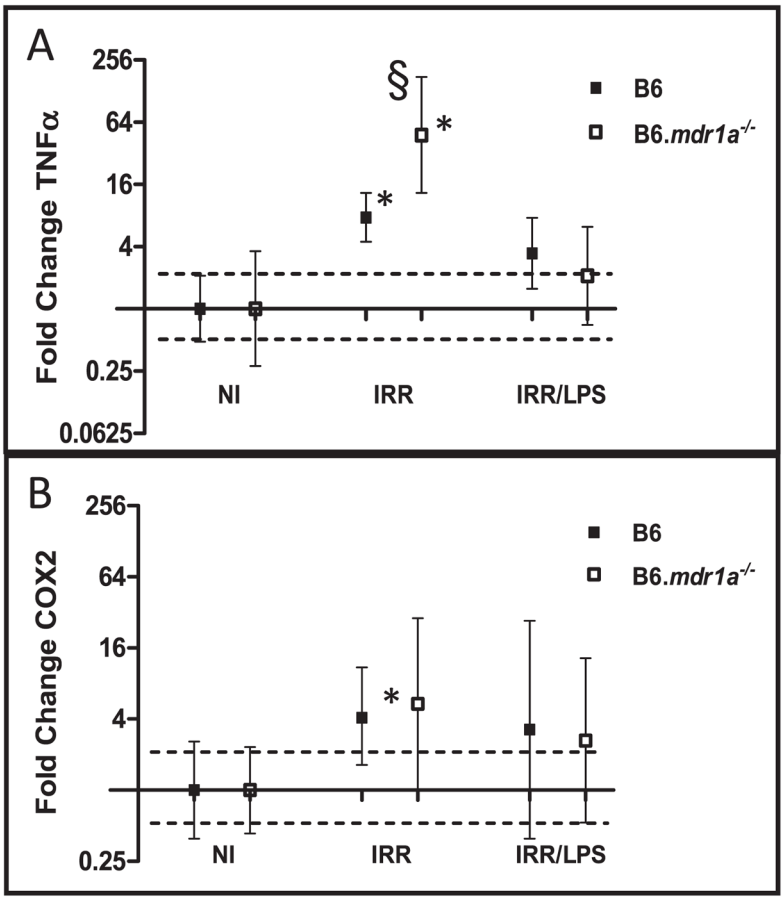

FIG. 5.

Gene expression of TNFα and COX2. Gene expression data were derived as previously described. Gene expression of TNFα (panel A) and COX2 (panel B), are represented graphically. $N = 5$ animals for all groups except B6 irradiated LPS where $N = 3$. $^{*}P < 0.05$ when values are compared to each strains own baseline gene expression. $^{\S}P < 0.05$ between treated B6.*mdr1a*$^{-/-}$ and treated B6 control animals.

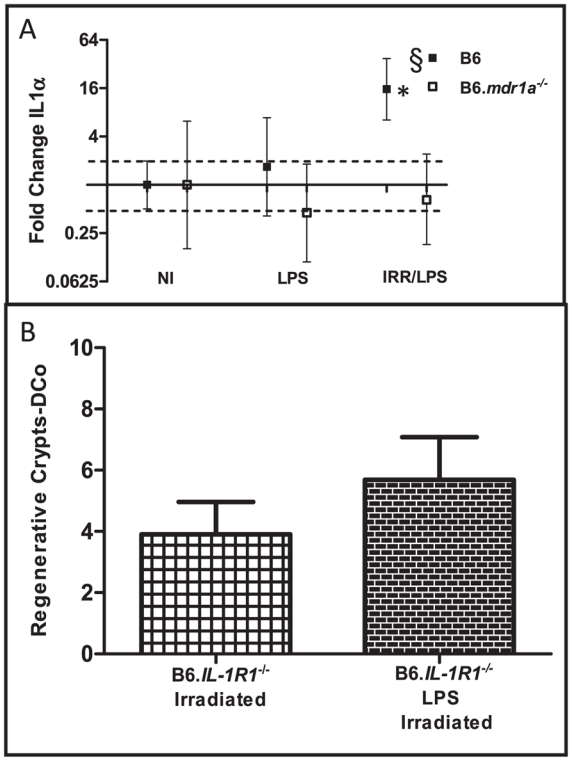

FIG. 6.

IL-1α gene expression and the effects of IL-1 signaling on LPS-induced radioprotection. RNA isolated from distal ileum (panel A). Distal colonic crypt regeneration was assessed in IL-1R1$^{-/-}$animals after exposure to radiation, with or without administration of LPS (panel B). $N = 5$ animals for all groups. *$P < 0.05$ when values are compared to each strains own baseline gene expression. $^{\S}P < 0.05$ between treated B6.*mdr1a*$^{-/-}$ and treated B6 control animals.